

Achievement of controlled resistive response of nanogapped palladium film to hydrogen

Cite as: Appl. Phys. Lett. **107**, 033108 (2015); <https://doi.org/10.1063/1.4927394>

Submitted: 24 April 2015 . Accepted: 14 July 2015 . Published Online: 24 July 2015

M. Zhao, M. H. Wong, and C. W. Ong



View Online



Export Citation



CrossMark

ARTICLES YOU MAY BE INTERESTED IN

[Self-assembled monolayer-enhanced hydrogen sensing with ultrathin palladium films](#)

Applied Physics Letters **86**, 203104 (2005); <https://doi.org/10.1063/1.1929075>

[The transition in hydrogen sensing behavior in noncontinuous palladium films](#)

Applied Physics Letters **97**, 121911 (2010); <https://doi.org/10.1063/1.3491263>

[Ultralow-power hydrogen sensing with single palladium nanowires](#)

Applied Physics Letters **94**, 223110 (2009); <https://doi.org/10.1063/1.3132064>

Lock-in Amplifiers

Find out more today



Zurich Instruments

Achievement of controlled resistive response of nanogapped palladium film to hydrogen

M. Zhao,¹ M. H. Wong,² and C. W. Ong^{2,a)}

¹Research Center for Solid State Physics and Materials, School of Mathematics and Physics, Suzhou University of Science and Technology, Suzhou 215009, People's Republic of China

²Department of Applied Physics and Materials Research Center, The Hong Kong Polytechnic University, Hung Hom, Kowloon, Hong Kong

(Received 24 April 2015; accepted 14 July 2015; published online 24 July 2015)

Palladium (Pd) film containing nanogaps of well controlled dimension was fabricated on a Si wafer having a high-aspect-ratio micropillar. The Pd film was arranged to experience hydrogen (H₂)-induced volume expansion. (i) If the nanogap is kept open, its width is narrowed down. A discharge current was generated to give a strong, fast, and repeatable on-off type resistive switching response. (ii) If the nanogap is closed, the cross section of the conduction path varies to give continuous H₂-concentration dependent resistive response. The influence of stresses and related physical mechanisms are discussed. © 2015 AIP Publishing LLC. [<http://dx.doi.org/10.1063/1.4927394>]

Palladium (Pd) exhibits substantial volume expansion when reacting with hydrogen (H₂).¹ This mechanism is used to close the nanogaps in some Pd-based substances for producing on-off type resistive response.^{1–6} Published results reflect some problems as follows. First, the device is required to give a sharp response at a target H₂ concentration. This further requires well control of the dimension and location of the Pd nanogaps.⁷ However, in many studies, the Pd nanogaps were generated by stress-induced cracking through repeated H₂ loading-unloading cycles,^{1,3,6,8–10} or by stresses relaxation in thin film.^{2,11–15} These nanogaps are non-uniform and exhibit random distributions. The responding behavior is hardly controlled and predicted. Second, the sensing behavior of a nanogapped Pd sensor may shift in repeated operation due to stress-induced successive deformation.^{6,9,16,17} A possible solution is to use a flexible substrate to fabricate thin film-type device to reduce the influence of the stresses.³ Third, the research-oriented fabrication techniques employed so far are hardly scaled up for mass production, like focused ion beam which is well known to have a very low yield rate.¹⁸

We report an approach aiming at alleviating the above problems. The method is to deposit a Pd film on a silicon (Si) wafer having a vertical high-aspect-ratio and rectangular-cross-sectioned Si micropillar. The Pd film is discontinuous at the gaps on the two sides of the Si micropillar. This approach allows accurate control of the width of the gaps and the thickness of the Pd film by means of micro-fabrication and thin film deposition techniques. The E-field inside the Pd gaps is highly adjustable to determine the desired electrical transport mechanism across the gaps and hence the H₂ detection behavior. Furthermore, the flexural compliance of the Si micropillar could help to reduce the influence of the stresses generated in the structure, such that the cyclic stability could be improved. The process also facilitates scaling up for mass production. The resistive response to H₂, the response time, and recovery time of the

samples were measured using a self-designed system to verify the validity of the idea.¹⁹

To fabricate a sample, a Si micropillar with a slim rectangular cross section was first produced as follows. First, a 1.1- μm thick thermal oxide was grown on a (100) Si wafer. Two narrow windows were opened on the oxide using photolithography and dry etching [Figs. 1(a) and 1(b)]. Deep reactive ion etching was applied to deep cut the Si under the windows. A Si micropillar of width $l_{\text{Si},x} = 1.57 \mu\text{m}$, length $l_{\text{Si},y} = 1 \text{ mm}$, and height $l_{\text{Si},z} = 75 \mu\text{m}$ was formed. The height-to-width ratio was 48. The inset in Fig. 1(b) shows the residual SiO₂ on the top of the micropillar. The widths of the left and right gaps, $l_{\text{L-gap},x}$ and $l_{\text{R-gap},x}$, are 2.6 μm and 2.0 μm , respectively [Fig. 1(c)]. Second, a 2.7- μm thick SiO₂ layer was sputtered on top to narrow down $l_{\text{L-gap},x}$ and $l_{\text{R-gap},x}$ to 900 nm and 430 nm in a controllable manner [Figs. 1(d) and 2]. The inset of Fig. 1(e) shows that the SiO₂ at the micropillar's tip exhibits a mushroom-like cross section. Third, a pair of 50-nm gold/5-nm chromium (Au/Cr) electrodes was fabricated on the two sides of the gaps using lift-off technique [Fig. 1(e)]. At last, a Pd layer was sputtered across the electrodes. The widths of the two gaps were further reduced in a linearly manner according to the thickness of the sputtered Pd (Fig. 2). Two sample types, denoted as Type I and II in the following, were produced according to the configuration of the gaps.

A Type I sample has a 1350-nm thick Pd layer on top. The as-fabricated configuration is indicated in Figs. 1(f) and 2. The gap on the right side was effectively closed ($l_{\text{R-gap},x} = 0 \text{ nm}$). The gap on the left remained open with $l_{\text{L-gap},x} = 300 \text{ nm}$. A high resistance $> 10 \text{ G}\Omega$ across the electrodes was observed at the as-fabricated state. A bias of 1 V was applied across the electrodes in the measurement to set up an E-field of $3.3 \times 10^6 \text{ Vm}^{-1}$ around the breakdown field strength of air. The resistance is expected to drop if the gap size is reduced for some reasons.

After the first exposure cycle to 4% H₂ (mixed in air) and followed by returning to air, the resistance across the gaps of the Type I sample dropped to $2.1 \times 10^4 \Omega$, which was

^{a)}Author to whom correspondence should be addressed. Electronic mail: c.w.ong@polyu.edu.hk. Tel.: (852) 2766 5689. Fax: (852) 2333 7629

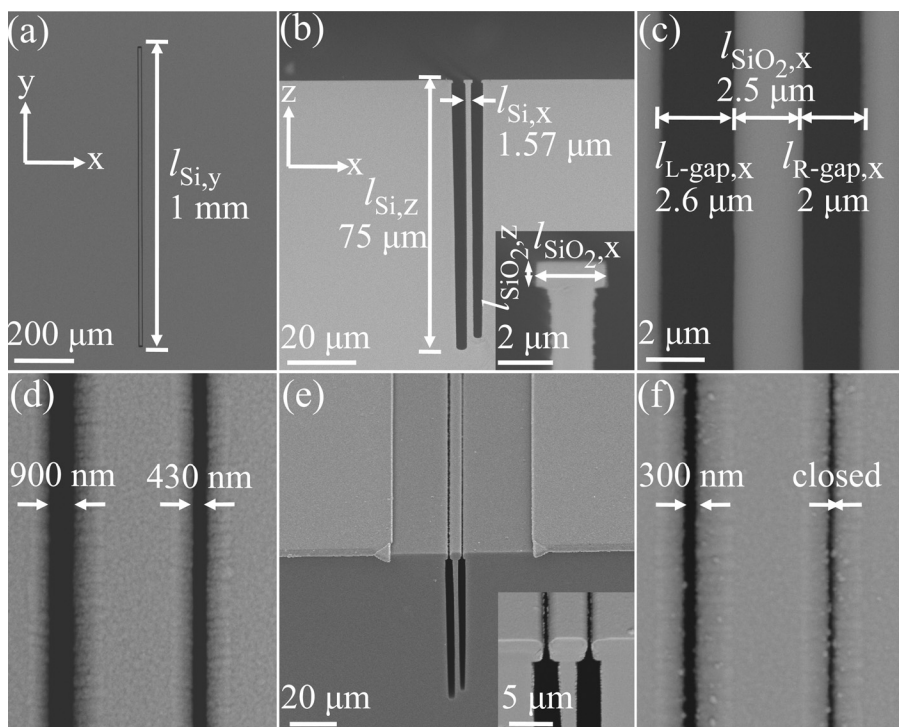


FIG. 1. (a) and (c) Top view of the micropillar covered by a thermal SiO_2 . (b) Cross-section of the micropillar. Inset: cross section of the thermal SiO_2 at the top of the micropillar and undercut of the micropillar's walls. (d) Top view of the micropillar with sputtered SiO_2 and reduced gap widths. (e) After the Au/Cr electrodes are added. Inset: cross section of the sputtered SiO_2 exhibiting a mushroom-like geometry. (f) Further reduction of gap size after the deposition of the Pd film.

much lower than the as-fabricated value of $10\text{ G}\Omega$. We notice an argument claiming that during hydrogenation of a Pd film adhered strongly to a substrate, Pd atoms are mainly driven to migrate in the direction perpendicular to the film surface,^{11,20} namely, out-of-plane expansion dominates. Accompanied by stress relaxation, out-of-plane plastic deformation occurred,^{20,21} which cannot be completely recovered after returning to the air environment. Furthermore, the film surface became rougher with the presence of some protrusions.²⁰ We suggest the following scenario. Referring to Fig. 3(a), the Pd layer in Region I expanded mainly in the z-direction during hydrogen loading. However, the Pd layer in Regions II and III can expand in both the x- and z-directions, which narrowed the width of the gap on the left side. The narrowing was not completely recovered after hydrogen unloading. The E-field in the gap, under a bias of 1 V, can

exceed the breakdown field strength of air to initiate discharge effect. A lower resistance of $2.1 \times 10^4 \Omega$ was thus observed, corresponding to a discharge current of $48 \mu\text{A}$. Referring to a published patent,²² a similar discharge current of 100 nA – $100 \mu\text{A}$ was found to be generated across a 50 – $100 \mu\text{m}$ wide air gap lying between an array of metal nanowire tips having diameters $\approx 200\text{ nm}$ and a metal plate under atmospheric pressure and a low voltage bias condition. The discharge current was claimed to be sensitive to the applied E-field.

Fig. 3(b) shows the H_2 concentration dependence of the resistive response of a Type I sample measured at 60°C . For H_2 concentration in the range of 1% – 3% (in air), the response is very weak, and H atoms are mainly dissolved in an α -Pd-H phase where the expansion of the lattice constant does not exceed 0.116% (from 0.38895 nm to 0.3894 nm). Referring to Figs. 1(d) and 1(f), the total thickness of the Pd layer located around the gaps on the two sides of the Si micropillar (Regions II and III) is $(900 + 430)\text{ nm}$ – $300\text{ nm} = 1030\text{ nm}$. If out-of-plane expansion of Pd dominates during H loading, this part of the Pd layer can only extend into the gap (in x-direction) by $1030\text{ nm} \times 0.116\% = 1.2\text{ nm}$. The narrowing of the gap width is thereby very tiny, such that the E-field and the discharge current in the gap are just slightly affected. If 4% H_2 is used, the resistance change is much more pronounced (from $21\text{ k}\Omega$ to $25\text{ }\Omega$). At this condition, an α -to- β phase transition occurs, where expansion of lattice constant can be as large as 3.36% (0.3894 nm to 0.4025 nm), giving rise to a total volume expansion of 10.82% . The Pd layer in Regions II and III can be thickened by $\approx 1030\text{ nm} \times (10.82\%/2) = 55.7\text{ nm}$. We further consider that such a narrowing is not large enough to close the gap which is originally 300 nm wide [Fig. 1(f)]. However, the E-field in the gap was enhanced by more than 22% . According to Ref. 22, such a percentage

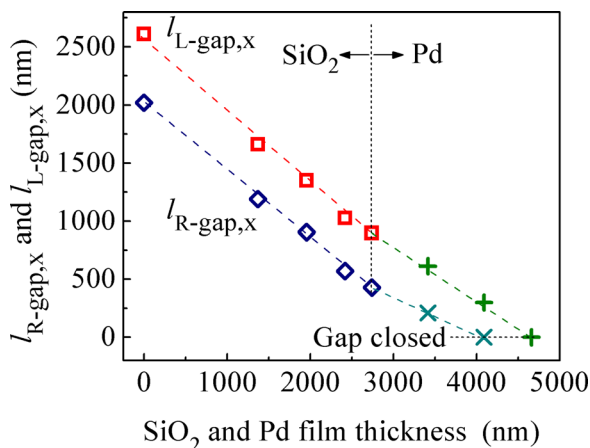


FIG. 2. Reduction of the gap widths ($l_{\text{R-gap},x}$ and $l_{\text{L-gap},x}$) against the total thickness of the SiO_2 and Pd layers.

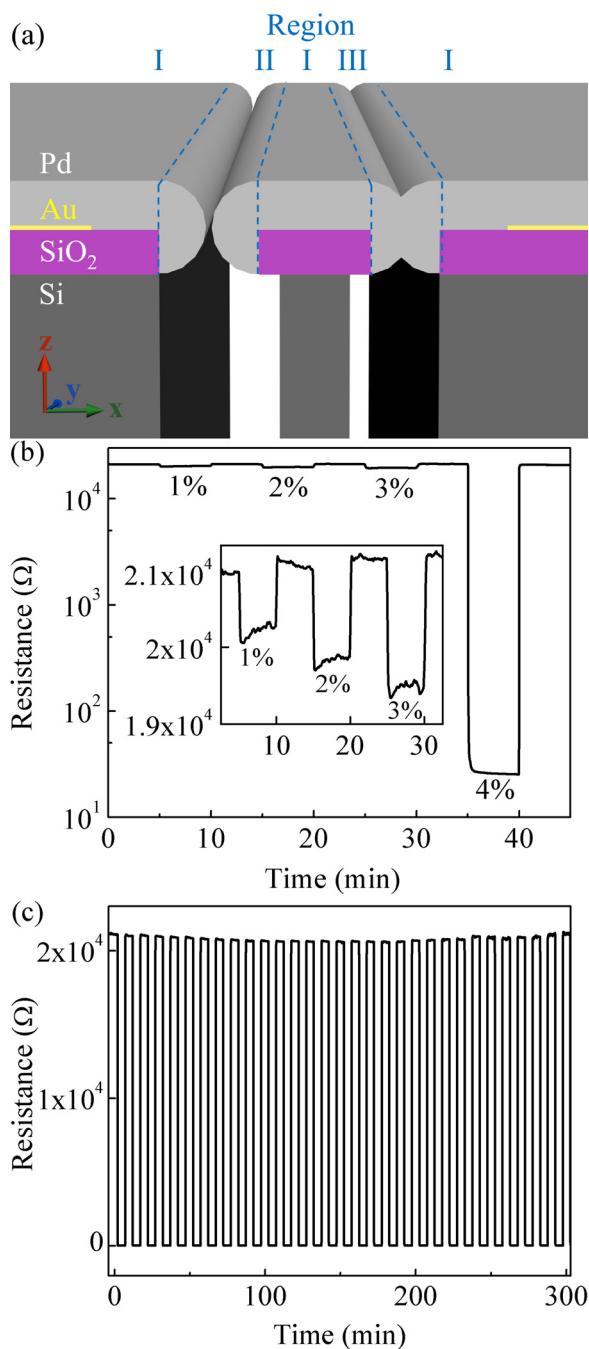


FIG. 3. (a) Schematic illustration of the cross section of the sample. (b) Resistive response of a Type I sample exposed to H₂ concentrations over 1%–4% in air at 60 °C. (c) Cyclic resistive response of a Type I sample when exposing to 4% H₂/air and air alternately at 60 °C.

increase in E-field can increase the discharge current crossing a narrow air gap by > 1000 times. This explains the sharp resistance change observed at 4% H₂. We further note that the threshold H₂ concentration observed in our study ($\approx 4\%$ at 60 °C) fits well to a temperature dependence of threshold H₂ concentration triggering α -to- β transition of Pd hydride as reflected by the data reported by individual authors.^{23,24} The threshold H₂ concentration is found to increase with increasing temperature, suggesting that the process is thermally unfavorable.

Cyclic test for the Type I sample was performed by exposing it to 4% H₂/air and air alternately at 60 °C. The

film resistance was switched between 25 Ω and 21 kΩ in a repeatable and stable manner [Fig. 3(c)]. The response time t_{res} and recovery time t_{rec} are <0.3 s and ≈ 3 s throughout the test. The stability of the response leads to the following inferences. (i) During H loading, the micropillar is driven to bend towards the left due to the expansion of the Pd lying in Region III. The force associated with the bending is $3E_{\text{Si}} \times I \times \Delta x / (l_{\text{Si},z})^3 \approx 5.6 \times 10^{-4}$ N, where $E_{\text{Si}} = 200$ GPa is the Young's modulus of silicon, $I = l_{\text{Si},y} \times (l_{\text{Si},x})^3 / 12$ the second moment of the micropillar, and $\Delta x = 300$ nm the maximum horizontal displacement of the micropillar tip. It creates a compressive stress ≈ 4.6 MPa in the Pd, which is much lower than the compressive strength of Pd-H (≈ 100 MPa) and cannot produce further plastic deformation.²¹ Stability of the cyclic response was thus achieved. (ii) The conduction process occurring in the gap for generating the resistive signal should not be a brush or arc discharge. Otherwise, the resistive signal would deteriorate quickly and very unstable. We further suggest that conduction process should be similar to a corona discharge process which is much gentler and less damaging.

The above arguments are further supported by the H₂-induced resistive response of the Type I sample observed at lower temperatures of 20 °C and 40 °C (Fig. 4). The main results are as follows. (i) The resistance drop in a hydrogen loading process has two stages. At 20 °C, the resistance drops slowly in the first stage, and accelerates in the second stage at ≈ 45 s after the commencement of the load process. At 40 °C, the second stage commences earlier, i.e., ≈ 3 s. At 60 °C, the two stages are hardly distinguished. The first stage is attributed to dissolution of H atoms into the α -Pd-H phase. The modulations of E-field and discharge current are little. The second stage is associated with the α -to- β transition involving a much larger lattice expansion, where the main resistance response is caused. (ii) The overall response time t_{res} and the recovery time t_{rec} are considerably shorter at higher temperature, e.g., t_{rec} drops from 1 h at 20 °C to 3 s at 60 °C. We attribute this effect to the larger diffusion rate of the reactant species.²⁵ (iii) The resistive response is weaker at a higher temperature. According to Sieverts' law, the H-to-Pd ratio in a Pd hydride is $(\text{H/Pd})_{\text{at}} = K_s \times (P_{\text{H}_2})^{\text{constant}}$,

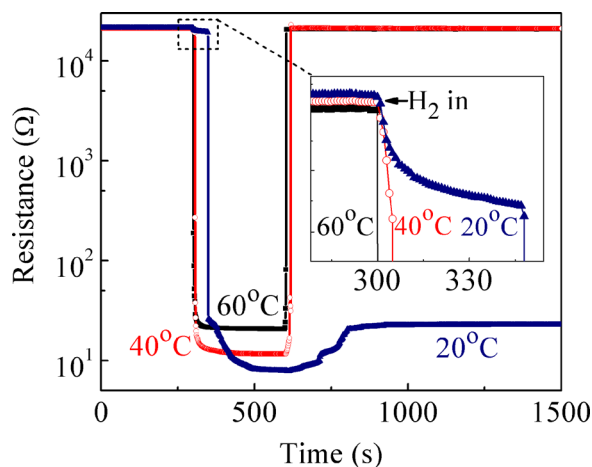


FIG. 4. Resistive response of a Type I sample exposed to 4% H₂/air and then air at 20, 40, and 60 °C.

where P_{H_2} is the H_2 partial pressure, and K_s the Sieverts constant. K_s depends on temperature T in the form of $\ln K_s = \Delta_s S/R - \Delta_s H/(RT)$, where $\Delta_s S$ and $\Delta_s H$ are the entropy and enthalpy of the loading process and R is the gas constant. If $\Delta_s H$ is negative, a higher T reduces K_s and $(H/Pd)_{at}$, and hence, a smaller resistive response is achieved. (iv) A Type I sample is more durable in repeated use compared to the one requiring direct contact as it relies on a non-contact mild discharge mechanism where wear and tear can be avoided.

A Type II sample has a 1920-nm thick Pd film. Both the gaps beside the micropillar were closed at the as-fabricated

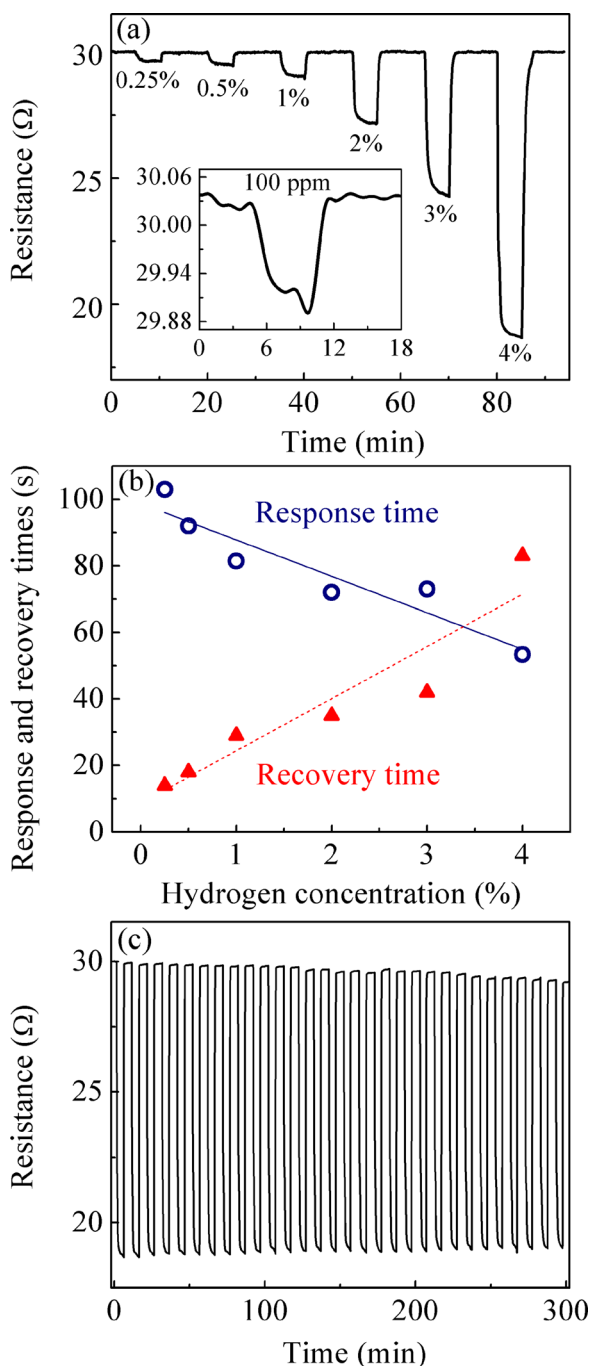


FIG. 5. (a) Resistive response of a Type II sample exposed to various H_2 concentrations. (b) Response and recovery times against H_2 concentration. (c) Results of a cyclic test obtained by exposing the sample to 4% H_2 in air and synthetic air alternatively.

stage (Fig. 2). The initial resistance between the electrodes was as low as 30Ω because a conduction path had formed initially. Out-of-plane (z -direction) Pd expansion occurs during hydrogenation, which is not different from what experienced by a Type I sample. Due to specific configuration of the nanogap, a Type II sample exhibits very different responding behaviors as follows. (i) Fig. 5(a) shows that the resistance changes continuously with H_2 concentration in a range of 100 ppm-4%. This is different from an on-off type switching behavior of a Type I sample. The lower detection limit is ten times better than the target to be achieved for a sensor used in monitoring H_2 leakage in a H_2 -powered vehicle. On the other hand, H_2 above 4% should also be detected by both types of samples based on H-induced expansion of the β -phase. (ii) The fractional response is prominently smaller than that of a Type I sample. For example, it gives a 60.4% resistance change at 4% H_2 in air instead of a change of three orders of magnitude given by a Type I sample. (iii) Fig. 5(b) shows that both t_{res} and t_{rec} are continuous functions of H_2 concentration. At a higher H_2 concentration, t_{res} is shorter but t_{rec} is longer. These features are determined by the diffusion processes under respective boundary conditions. (iv) The response relies on real contact such that the cyclic stability is not as good as that of a Type I sample [Figs. 5(c) and 3(c)].

In summary, a Pd film deposited on a Si wafer having a high-aspect-ratio micropillar contains nanogaps of well controllable dimensions. Two different types of resistive response were achieved, which were all based on H_2 -induced Pd volume expansion effect. When the gaps are not completely closed, H_2 concentration affects the gap width to give a strong, fast, and repeatable on-off resistive response via a corona-like discharge mechanism. When the path is closed by Pd, H_2 concentration affects the cross-sectional area of the conduction path to give a relatively weak continuous resistive response over a broad H_2 concentration range. Both structures exhibit improved controllability, stability, and mass producibility, and can be integrated together to form sensor array of extended dynamic range.

The work described in this paper was supported by Research Grants Council of the Hong Kong Administrative Region (Project Nos.: PolyU 5016/08P and PolyU 5242/11E, Account codes: B-Q10N and B-Q26D), the NSF of China (Project No.: 11374225) and Innovative Technology Fund (Project No.: ITS/558/09, ZP2U, Account code: K.11.27.ZP2U).

¹F. Favier, E. C. Walter, M. P. Zach, T. Benter, and R. M. Penner, *Science* **293**, 2227 (2001).

²T. Xu, M. P. Zach, Z. L. Xiao, D. Rosenmann, U. Welp, W. K. Kwok, and G. W. Crabtree, *Appl. Phys. Lett.* **86**, 203104 (2005).

³J. Lee, W. Shim, E. Lee, J. S. Noh, and W. Lee, *Angew. Chem. Int. Ed.* **50**, 5301 (2011).

⁴T. Kiefer, L. G. Villanueva, F. Fargier, F. Favier, and J. Brugger, *Nanotechnology* **21**, 505501 (2010).

⁵L. G. Villanueva, F. Fargier, T. Kiefer, M. Ramonda, J. Brugger, and F. Favier, *Nanoscale* **4**, 1964 (2012).

⁶C. W. Ong and Y. M. Tang, *J. Mater. Res.* **24**, 1919 (2009).

⁷J. Lee, W. Shim, J. S. Noh, and W. Lee, *ChemPhysChem* **13**, 1395 (2012).

⁸B. Jang, K. Y. Lee, J. S. Noh, and W. Lee, *Sens. Actuators, B* **193**, 530 (2014).

- ⁹E. C. Walter, F. Favier, and R. M. Penner, *Anal. Chem.* **74**, 1546 (2002).
- ¹⁰F. Yang, D. K. Taggart, and R. M. Penner, *Nano Lett.* **9**, 2177 (2009).
- ¹¹O. Dankert and A. Pundt, *Appl. Phys. Lett.* **81**, 1618 (2002).
- ¹²M. Khanuja, D. Varandani, and B. R. Mehta, *Appl. Phys. Lett.* **91**, 253121 (2007).
- ¹³T. Kiefer, L. G. Villanueva, F. Fargier, F. Favier, and J. Brugger, *Appl. Phys. Lett.* **97**, 121911 (2010).
- ¹⁴J. van Lith, A. Lassesson, S. A. Brown, M. Schulze, J. G. Partridge, and A. Ayesh, *Appl. Phys. Lett.* **91**, 181910 (2007).
- ¹⁵B. Xie, M. Y. Zheng, F. Liu, X. Peng, G. H. Wang, and M. Han, *J. Nanopart. Res.* **15**, 1746 (2013).
- ¹⁶R. Gremaud, M. Gonzalez-Silveira, Y. Pivak, S. de Man, M. Slaman, H. Schreuders, B. Dam, and R. Griessen, *Acta Mater.* **57**, 1209 (2009).
- ¹⁷E. Lee, J. M. Lee, J. H. Koo, W. Lee, and T. Lee, *Int. J. Hydrogen Energy* **35**, 6984 (2010).
- ¹⁸T. Kiefer, F. Favier, O. Vazquez-Mena, G. Villanueva, and J. Brugger, *Nanotechnology* **19**, 125502 (2008).
- ¹⁹M. Zhao, J. X. Huang, M. H. Wong, Y. M. Tang, and C. W. Ong, *Rev. Sci. Instrum.* **82**, 105001 (2011).
- ²⁰Y. Pivak, H. Schreuders, M. Slaman, R. Griessen, and B. Dam, *Int. J. Hydrogen Energy* **36**, 4056 (2011).
- ²¹E. Dillon, G. Jimenez, A. Davie, J. Bulak, S. Nesbit, and A. Craft, *Mater. Sci. Eng. A* **524**, 89 (2009).
- ²²J. Mazher, S. Ghosh, and P. Ayyub, International patent No. WO2008/029416-A1 (March 13, 2008).
- ²³F. A. Lewis, *The Palladium Hydrogen System* (Academic Press, London, 1967), p. 19.
- ²⁴D. Yang, L. Valentín, J. Carpena, W. Otaño, O. Resto, and L. F. Fonseca, *Small* **9**, 188 (2013).
- ²⁵F. Yang, D. K. Taggart, and R. M. Penner, *Small* **6**, 1422 (2010).